Development of tools to study human hair follicle biology in vitro - focus on hair follicle stem cells and their potential application in Vitiligo therapy

Maria Henriques[1,2,*]

Thesis to obtain the Master of Science Degree in Biomedical Engineering – November 2017

Supervisors: Prof. João Ferreira[2] and Prof. Cláudia da Silva[1]

[1]Instituto Superior Técnico, University of Lisbon, Portugal; [2]Instituto de Medicina Molecular, Faculty of Medicine, University of Lisbon, Portugal; *Email: maria.adegas.henriques@tecnico.ulisboa.pt

ABSTRACT: The study of human hair follicle (HF) dynamics is a key point to find more effective treatments for skin disorders such as Vitiligo. Human HF cycle and skin stem cells are a particularly interesting field, since HFs cycle continuously and stem cells have a crucial role in this phenomenon. Most of the studies addressing HF dynamics were performed in animals, so these results cannot be directly translated to humans. The present master thesis aims to contributing to fill-in this gap through the development of tools to study human HF biology. In this context, a tool for cell cycle quantification using microscopy was successfully developed using HCT-116 cells exposed to 5-Ethynyl-2'-deoxyuridine (EdU), whose signal was measured using *CellProfiller* software. S-phase was estimated to last 6/7h, G1-phase 4/5h and G2-phase 4/5h. Additionally, a method for analyzing human HF dynamics was established and EdU-positive cells were quantified (labeling index) in diverse HF regions. As expected, the bulb region showed the highest labeling index, but proliferation in outer root sheath cells was also documented and quantified. Lastly, the initial steps to obtain isolated HF stem cells were also performed. The protocol for obtaining HF epithelial cell suspensions from human biopsies was established after an optimization process, with CnT-07 medium proving appropriate for culture of these cells. The tools developed in this master thesis will be used in the future to pursue our aim of implementing cell therapies for patients suffering from Vitiligo.

KEYWORDS: *Skin stem cells; Cell cycle; Hair follicle; Proliferation, Microscopy.*

1. INTRODUCTION

Vitiligo is a chronic pigmentary disorder which manifests as circumscribed white macules or patches in the skin and in mucous membranes, in areas where there was loss of melanocytes[1]. Over time, several pathophysiological theories emerged, with the aim of explaining the cause of this disease, such as neurohumoral, autoimmune and intrinsic theories[2]. However the exact cause(s) of Vitiligo remain(s) elusive[1][3]. This lack of information makes the disease management harder. Nowadays, there are diverse types of treatment, however any presents ideal results[3][4]. Many researchers have been developing treatments based on hair follicle stem cells (HFSCs), where cell suspensions are transplanted into Vitiligo lesions (Cellular Grafting)[5]. HFSCs reside on the bulge region of the hair follicle, and give rise to a population of cells which rapidly divide in the matrix, named the transit-amplifying cells[6]. In fact, since 1991 when Cui and co-workers proved the role of HFSCs, more specifically, Melanocyte stem cells (MSCs) on vitiligo repigmentation, that is known that these cells are a key aspect for developing an effective therapy for Vitiligo. More specifically they understood that active melanocytes were absent on Vitiligo patients, however the amelanotic melanocytes on bulge (MSCs) were undamaged[7]. In addition, it is known that MSCs maintain their quiescence state until being activated by a stimuli, become transit-amplifying cells and differentiate into melanocytes that produce melanin[8]. In 2011 Mohanty and colleagues tested the efficacy of Cellular Grafting on 14 patients with stable Vitiligo. For this purpose, they applied the cell suspension on dermabraded recipient areas. They observed that 9 of 14 patients presented repigmentation above 75%[9]. The results of this techniques are still not ideal. Consequently, useful tool for better understand human hair follicle (HF) dynamics have been described in the literature[10]. Label-retaining methods have been described for identify specific stem cell populations, through the incorporation of nucleotide analogues such bromodeoxyuridine (BrdUrd) or tritiated [3H]thymidine into newly synthetized DNA. Stem cells are characterized by a slow cycling nature, thus by studying the retention of label within these cells allows their identification (Label Retaining Cells – LRCs)[11]. In 1990 Cotsarelis and colleagues incorporate tritiated [3H]thymidine into mice and after one week researchers identified labeled cells in a specific area of the hair follicle, the bulge region[6]. However, label-retaining methods did not allow the identification of a wide range of cell populations, so several markers for specific HF regions and HF cell populations have also been utilized[12]. In 1998 Lyle and colleagues transplanted human skin into mice (xenotransplantation) for study bulge cells. Firstly, they performed immunohistochemistry using the monoclonal antibody C8/144B,

which predominantly identified bulge cells. After characterizing the C8/144B antibody as specific for cytokeratin (CK) -15, they identified the presence of typical stem cell features on cells labeled with CK-15, as slowly cycling and proliferative behavior at the beginning of anagen. Those findings highlighted that CK-15 may be used as a marker of HFSCs[13]. Cell surface markers with significant specificity have also been identified. In 2006, Ohyama and colleagues identified surface proteins which are candidates to be stem cells markers. More specifically, they performed a microarray analysis to obtain the gene expression profiles of ORS cells. They identified CD200 as a surface marker with high specificity to bulge area. In addition, other surface markers were identified as surface proteins that are overrespresented in certain ORS areas namely CD24 in the inner bulge, CD34 in suprabulbar region and CD71 in both sub-bulge and suprabulbar regions[14].

Cell cycle dynamics have also been studied as an essential phenomenon HF growth. In addition, studying cell cycle of HF cells in the perspective of Vitiligo can give important insights regarding its pathophysiology[15]. Cell cycle is the set of events that happen between two mitoses. Proliferating cells are in cycle and pass through several cell cycle phases: the growth phase after mitosis or interphase (G1-phase), DNA synthesis (S-phase), resting or pre-mitotic growth phase (G2-phase) and mitosis[16]. Cell cycle dynamics have been studied through quantification of their stages which relies on labeling cells with DNA stains and/or specific stains, as nucleosides analogues that label cells in specific cell cycle phases such as S-phase. Measurement of DNA content allows understanding the frequency of cells present in each cell cycle phase, since DNA content of G1 and G2 cells is respectively 2n and 4n[17][18]. [3H]thymidine and BrdU have been widely used in cell cycle studies to stain cells in S-phase. However [3H]thymidine technique provides low resolution, is slow and induces DNA damage. Although BrdU technique is faster, can promote cytostatic effects and requires a DNA denaturation step to allow anti-BrdU antibodies to reach BrdU epitopes, which is harsh to DNA and can promote structure degradation. 5-Ethynyl-2'-deoxyuridine (EdU) is an analogue of thymidine used as an alternative to [3H]thymidine and BrdU[19][20]. Flow cytometry is the gold standard technology used for cell cycle quantification, since it provides a fast and truthful cell cycle analysis[18][21]. Namely, this year (2017) Pereira and colleagues developed a tool for quantitative assessment of the cell cycle by flow cytometry, termed E-CFI (EdU-coupled fluorescence intensity analysis)[22]. Although many studies have been shown the efficiency and accuracy of this method, some researchers have been struggling with the requirement of specific instrumentations, and knowledge and experience with this technology[21]. In order to overcome this issue, in the past years some investigators have tried to find an alternative to this technique. Quantification of cell cycle using Fluorescence Microscopy has been studied and seems to be an accurate alternative to flow cytometry[21][23]. One advantage of microscopy in contrast to flow cytometry in the case of tissues is the possibility of maintain spatial context, that is, the natural architecture of samples [23]. In one study published in 2015 by Roukos and co-works, these researchers developed a protocol for determining cell cycle staging through measuring DNA content, using two different fluorescence microscopies: High-throughput confocal microscopy and Widefield microscopy[21]. In 2017, Ferro and colleagues also reported the use of microscopy to acquire DNA content but using a different method for image analysis[23].

Besides using nucleosides analogues to study the cell cycle of specific isolated cells, as previously described, researchers have used these labels, in addition to others, for characterizing proliferation patterns in biological tissues such as the HF [24]. In 2009, Kloepper and colleagues developed a classification system for distinguish human HFs in anagen IV from early catagen. Subsequently, qualitative and quantitative criteria were stablished using DAPI (DNA stain), Ki-67 (to identify cycling cells) and TUNEL (which identifies apoptotic cells) [25]. In 2016, Purba and colleagues developed a primer for studying cell cycle dynamics in human HF and mentioned EdU as a useful S-phase marker. They used sections of human HFs, previously incorporated with EdU, to performed immunofluorescence experiments. They evidenced the potential of EdU alone or in a double stain, for distinguish different cell populations[15].

Furthermore, the isolation and expansion of HFSCs have been investigated in order to develop clinical treatments based on regenerative medicine for skin diseases such as Vitiligo. In 2006, Ohyama and colleagues isolated human HFSCs by combining positive and negative markers of bulge cells[14]. More recently(2013), Hilmi and colleagues also developed a culture method for epithelial stem cells derived from human hair follicles and highlighted the potential of CnT07 culture media for culturing these cells[26].

It is evident the variety of interesting fields that can give important insights regarding human hair follicle dynamics in healthy people and also in the perspective of Vitiligo. The need for a novel therapy for this disease combined with the obvious potential of HFSCs has motivated research on this area. Th is master thesis intents to contribute to this research. For this purpose, the aims of the study are: developing a relatively fast and user-friendly tool for cell cycle quantification using microscopy, which can be applied to sectioned human HFs; development of a quantitative method for analyzing human HF proliferation in vitro, which can be applied to disease models such as Vitiligo and/or adapted to other labels to easily study other features besides proliferation; and initiating the work leading to HFSCs isolation.

2. MATERIALS AND METHODS

2.1. Cell cycle quantification using EdU

2.1.1. Cell culture and EdU incorporation

Human colorectal carcinoma HCT-116 cells were cultured in RPMI 1640 (Gibco®) medium, supplemented with 10% foetal bovine serum (FBS), 2mM L-glutamine, 10 mM MEM non-essential amino acids and 100U/ml penicillin/ streptomycin (all from Gibco®), and maintained at 37ºC, 5%CO2. The medium was changed every 2-3 days, and cells were passaged when sub-confluent to petri dishes containing glass coverslips. When cells growing onto coverslips reached a confluence of approximately 60-70% they were transferred to 30cm2 petri before exposure to EdU. EdU (10µM, from a stock of 10mM in DMSO) was added to parallel cultures for incremental periods of time (1h increments): time-points T0h until T8h or T10h. Cells not exposed to EdU were used as controls (T0Ah and T0h). Then, cells were fixed, for 16-72 hours with 4% formaldehyde (PBS, Sigma®).

2.1.2. EdU staining and whole DNA staining

Firstly, the cells were washed three times with Elix® water. After increasing the permeability of cells with 70% ethanol (5 minutes, room temperature) followed by 1% SDS (10 minutes, room temperature), cells were incubated for 20 minutes with the reaction cocktail prepared from the Click-iT® EdU Alexa Fluor® 488 Imaging kit (Invitrogen). One of the controls was also incubated

with the EdU detection system (T0h). After, they were incubated with the DNA stain: 1µg/mL 4',6-Diamidino-2-Phenylindole (DAPI, Sigma®) 4 hours in the dark; or 1µg/mL Hoechst 33342 (Click-iT® EdU Alexa Fluor® 488 Imaging kit – Invitrogen) 4 hours at room temperature; or 10 µg/mL Propidium Iodide (PI, Sigma®) overnight at 4ºC. Microscope slides were mounted in VECTASHIELD® medium (Vector Laboratories) and stored at -20ºC until used. After SDS incubation, cells were washed three times with PBS/0.05%Triton X-100 (Sigma®) between each step.

PI requires the removal of RNA using RNase A (Sigma®). After the steps of cellular permeabilization, cells were incubated with a solution of 500µg/mL RNase A in Tris 0.1M and 10mM MgCl2 for 45min at 37ºC. After washes with PBS/ 0.05%Triton X-100, 1%FA was added for 5 minutes to inactivate RNase A.

2.1.3. Image acquisition using Widefield Fluorescence Microscopy

Images of the cells were acquired using a Widefield fluorescence microscope *Zeiss Axio Observer*. Depending on the specific experience, either a single channel (Alexa 488) or a multi- channel (Alexa 488 and DAPI or Alexa 488 and Hoechst or Alexa 488 and PI) acquisition was utilized, using the filtersets DAPI, HE GFP and HE DsRed for DAPI, Alexa 488 and PI respectively. 12 images per time-point were acquired with a magnification lens of 20x, resolution of 2252 × 2208 pixels (624,7 × 501.22 µm) and pixel size of 0,227µm.

2.1.4. Image acquisition using Spinning Disk Confocal Microscopy

The spinning Disk Confocal Microscope 3i Mariana SDC was used to perform a single channel acquisition of Alexa 488. The laser unit used to excite the sample was the Laserstack 488. 12 z-stacks per time-point were acquired with a magnification of 20x, resolution of 512 × 512 pixels (341,33 µm × 341,33 µm) and pixel size of 0,667µm. Each z-stack comprised 49 slices whose maximum projections were generated to be used later.

2.1.5. CellProfiller software and RStudio for image analysis

CellProfiller software was used for identify the cells on the images and measure their intensities (Nuclei-txt)[27]. It works with projects that are composed by an image file list containing the images to be analyzed; a pipeline, the sequential set of modules that analyze input images; and optionally the metadata, that is the associated information about the images[28]. Then, *RStudio* was used to obtain the frequency of cells with each intensity, create the histograms (Fraction of cells vs Integrated Intensity), calculate the percentage of cells present in specific histogram regions (CellCycle_Percentages_table.txt) and calculate the frequency of cells for each binned value (CellCycle_BinnedFrequencies_table.txt). Microsoft ® Excel was used to perform calculations and GraphPad Prism 7.03 to obtain the final graphs.

2.1.5.1. CellProfiller Project 1 - Measuring intensity of EdU-positive cells

For selecting EdU-positive cells, in *NamesAndTypes* module, the channel of interest was chosen based on C number (that is an index given to each channel) present in images metadata. The set of modules used to analyze the images, identify the nuclei of cells and measure their intensities was the as follows: *IdentifyPrimaryObjects, MeasureObjectIntensity, MeasureObjectSizeShape, OverlayOutlines, DisplayDataOnImage, SaveImages* and *ExportToSpreadsheet*. The critical module is the *IdentifyPrimaryObjects* where the objects are identified. The typical diameter of objects selected was 40-75; the threshold strategy was *Global*; the thresholding method was *Otsu* and the method to distinguish clumped objects and draw dividing lines between them was *Shape*. The module MeasureObjectIntensity records several measurements of intensity such as *IntengratedIntensity* which is the measurement used in this thesis to analyze the signal within cells.

2.1.5.2. CellProfiller Project 2 - Measuring intensity of EdU-negative cells

To obtain EdU-negative cells, EdU-positive cells were eliminated. A correct elimination requires a extremely well identified. This stringency was only achieved using the *Manual* strategy to establish the threshold values.

Preliminary Project

A preliminary project was used to estimate the best threshold values suitable for each time-point and each channel. It was used the same set of analyse modules as Project 1, with different settings in *IdentifyPrimaryObjects* module. The Threshold Strategy used was *Manual* instead of *Global*, the range of typical diameter was broader (e.g. 38-90), and the method to distinguish clumped objects and the method to draw dividing lines between clumped objects were *Intensity* instead of *Shape*.

Main Projects

After obtaining the threshold values, the main project was constructed with two sub-projects (part 1 and part 2) which were run consecutively: part 1 where the images with the cells of interest (EdU-negative cells) were created and part 2 where the intensities of those cells were measured and recorded. The part 1 was constituted by the following set of modules: *IdentifyPrimaryObjects, IdentifyPrimaryObjects, MaskImage, MaskImage, ImageMath, ImageMath* and *SaveImages*. The *IdentifyPrimaryImages* modules identify the cells on each channel, using the threshold values selected on Preliminary Project, and a similar typical diameter (e.g.30-95). The module *MaskImage* hides certain parts of the input image, creating a mask. Two masked images were generated, one for each channel. Then, two ImageMath modules were used to eliminate cells. First an image with the cells to be eliminated was created using the mathematical operation And, and then these cells were subtracted to the image with total cells, using the operation Subtraction. Part 2 was constituted by the same set of modules as Preliminary Project, but with different settings on *IdentifyPrimaryObjects*. The range of typical diameter chosen became smaller again, the value of threshold used was the same as used in part 1 for this channel and the method to distinguish clumped objects and the method to draw dividing lines between them were *Shape* instead of *Intensity*.

2.1.5.3. R code

Rstudio was used to analyse the data obtained from *CellProfiller*. The inputs that need to be nomenated on the code were some specific information regarding the experiment and time-point in question, such as the location of Nuclei.txt and some information about the histograms, including the maximum value of xx axis, bin width and the dimensions of the output image. For each time-point, the directory of the file data was adapted, along with the corresponding time-point, indicated in the vector treat.levels. For each experiment, the name was also adapted. More specifically, this name was given to the images in the Main Project-part2.

2.1.6. Statistical analysis

Graphs with mean values display error bars which represent standard deviations. GraphPad Prism 7.03 does not draw the error bars when error bars are shorter than the height of the symbol.

2.2. Hair follicle characterization

2.2.1. EdU incorporation

Human scalp biopsies were obtained from *Hospital CUF Descobertas* and *Hospital de Santa Maria*. Culture media containing EdU were prepared through dilution of a stock of 10mM EdU in DMSO to a final concentration of 10 or 15 µM in ProCHO™ 4 medium (04-919Q, Bio Whittaker®, Lonza) supplemented with 2mM L-glutamine, and 100U/ml penicillin/streptomycin (both from Gibco®). Biopsies were incubated during 12h or 4h (experiment 1 and 2, respectively), at 37ºC, 5% CO2. After, biopsies were fixed in 4% FA in PBS at 4ºC, for 8 weeks and 6 days (experiment 1 and 2, respectively).

2.2.2. Preparation of samples, inclusion and sectioning

After several washes in PBS, human scalp biopsies were incubated at 4º C overnight in the hydrogel monomer solution A4P0 (4% (w/v) acrylamide in PBS), supplemented with 0.25% (w/v) photoinitiator 2,2'-Azobis(2-(2-imidazolin-2-yl) propane) dihydrocloride (VA-044, Wako Chemicals). Afterwards, the A4P0-infused samples were degassed with nitrogen for 1-5 minutes and incubated for 1-3 hours at 37ºC to initiate polymerization. Then, biopsies were washed with PBS and transferred into 50 mL Falcon tubes containing 8% (w/v) SDS in PBS (ph7.5), and they were incubated for 5hours at room temperature and 1h at 37ºC, with mild shaking. Biopsies were then incubated with 20% sucrose (Sigma®) in PBS during 16-48h. After, they were included and sectioned in the *Histology and Comparative Laboratory* of *Instituto de Medicina Molecular,* Lisbon.

2.2.3. EdU staining and Immunofluorescence

Sections were incubated 20 minutes with the reaction cocktail prepared from the Click-iT® EdU Alexa Fluor® 488 Imaging kit. For CK-15 staining, cells were incubated with a mouse primary antibody anti CK-15 (1:100, ab80522, abcam) for 1 hour at 37ºC and then incubated with a secondary antibody cy3 goat anti-mouse (1:100, abcam) for 1 hours at 37ºC. The signal was fixed with 2% FA in PBS for 10 minutes. Staining of DNA using DAPI or Hoechst 33342 (both 1µg/mL) was also performed for at least 4 hours at room temperature. Microscope slides were mounted in VECTASHIELD® and stored at -20ºC. Cells were washed three times with PBS/0.05%Triton X-100 (Sigma®) between each step.

2.2.4. Image acquisition using Confocal Point-Scanning (SD) Microscopy

The Confocal Point-Scanning Microscope *Zeiss LSM 710* was used for a multi-channel acquisition DAPI or Hoechst and Alexa 488, or DAPI or Hoechst and Alexa 488 and CK-15. A pinhole size of 2.1 ± 0.1 µm was used throughout all acquisitions. Whole DNA stain excitation was performed using a 405 nm line from the laser unit Diode 405-30, Alexa 488 excitation was performed using a 488 nm line from the laser unit Argon and CK-15 excitation was performed using a 561 nm line from the laser unit DPSS 561-10. Acquisition of images was performed for different anatomical areas of hair follicle (bulb, sub-bulge, bulge and supra-bulge), epidermis, and sebaceous gland, with a magnification of 20x or 10x, resolution of 1024 × 1024 pixels (708.49 × 708.49 µm or 1416.99 × 1416.99 µm respectively) and pixel sizes of 0,60 µm and 1,31 µm respectively.

2.2.5. Image analysis and quantification using *Fiji*

Hair follicle images were organized according to anatomical areas (bulb, sub-bulge, bulge and supra-bulge) before analysis. The image processing package *Fiji* was utilized herein for image processing. The cell counter plug-in was used to count cells stained with EdU in the bulb and sub-bulge regions. The remaining regions were qualitatively analysed, in the same way as the images of epidermis and sebaceous gland. Microsoft ® Excel was used to perform calculations and GraphPad Prism 7.03 to obtain the final graphs.

2.2.6. Orcein-Gimsa protocol

Microscope slides previously subjected to immunostaining were disassembled, washed in Elix® water and stained in Orcein (Merck) for 30 minutes. The background was reduced by a short immersion in 95% EtOH (Merck). After washing the sections with running water for 10 minutes, they were stained in 1% Gimsa (Merck) for 1h at room temperature. The excess of blue shades was removed by placing the sections in a 95% EtOH with some drops of eosin (Merck). In the end, they were mounted in DPX (gurr®) mounting medium. Images were acquired using a brightfield microscope *Leica DM2500*, with a magnification lens of 20× (pixel size=0,3µm).

2.2.7. Statistical analysis

Graphs with mean values display error bars which represent standard deviations. GraphPad Prism 7.03 does not draw the error bars when error bars are shorter than the height of the symbol.

2.3. Preparation of hair follicle cell suspension from human biopsies

Hair follicles biopsies were minced in approximately 1 mm fragments with the aid of a scalpel. Then the fragments were incubated in HBSS (Gibco®) supplemented with 1mg/mL collagenase/dispase (Sigma®), prepared from a stock of 10mg/mL in PBS, overnight at 37ºC. Fragments disruption was aided by vigorous pipetting, resulting in HFs separated from surrounding dermis. The HFs were then incubated with trypLE™ Express for 20-30 minutes at 37ºC. Afterwards, the disruption of epithelial cells from HFs was achieved by vigorous pipetting. TrypLE was quenched by adding of an equal volume of HBSS supplemented with 10% Fetal calf serum (Gibco®). Free cells and tissue debris were then centrifuged (350xg, 7 minutes) and subsequently resuspended in HBSS, passed through a 100 µM diameter mesh (cell strainer, Falcon) and centrifuged again as above. Free cells and small aggregates were then resuspended in 5mL of fully supplemented (as per manufacturer instructions) CnT07 medium88 (CellnTech[29]), additionally supplemented with 100U/ml penicillin/streptomycin (Gibco®) and incubated at 37ºC, 5% CO_2 . The media was changed every three days and cells were passaged when sub-confluent.

3. RESULTS AND DISCUSSION

3.1. Cell cycle quantification using Microscopy

The tool developed for cell cycle quantification through microscopy-based analyses was addapted from a previously one

that makes use of flow cytometry, termed E-CFI (EdU-coupled fluorescence intensity analysis)[22]. In addition, the method utilized for cell cycle quantification using microscopy was further adapted from a paper of Roukos et al. (2015), where they established a protocol for determining cell cycle staging through measuring DNA content using microscopy[21].

In all of the experiments DNA was labeled with EdU. Experiments 5 to 12 were also labeled for whole DNA with a DNA stain: PI (experiment 5 and 6), Hoechst (experiment 7) or DAPI (experiments 8 to12). Experiments 11 and 12 comprise two additional time-points (T9h and T10h). Finally, images in experiments 1 to 12 were all acquired using widefield microscopy, while images of experiments 13, 14 and 15 were acquired using SD confocal microscopy.

3.1.1. Estimation of S phase duration time

The estimation of S-phase duration time was performed according to the founder concept of the E-CFI technique – S phase duration equals the minimum time to reach maximum EdU-coupled fluorescence. For this purpose, the main goal of this analysis was to accurately identify the sufficient number of cells stained for EdU, and not identify cases of giant cells or cell clusters. So, the typical diameter range chosen was quite restrict and the method selected for distinguish clumped objects and draw dividing lines between them was *Shape*.

After running the R code, the histograms of Fraction of cells vs EdU Integrated Intensity, for each time-point (until T8h) of each experiment were obtained with a bin of 4, as well as the file with the frequencies of cells for each bin value. These graphs did not allow an easy and simple perception about the time point where the maximum intensity was achieved. So, the graphs Cumulative fraction of cells vs EdU *Integrated Intensity* were created, which are much more illustrative. The cumulative fraction of cells were estimated based on frequencies obtained from R code (CellCycle_BinnedFrequencies_table.txt). Since this analysis was performed based on Maximum Integrated Intensity values, the graph Maximum EdU Integrated Intensity vs time-points was as well created for each experiment. The maximum Intensity of each time-point is the lowest value of EdU Integrated Intensity for which the cumulative fraction of cells is approximately 1. Thus, these graphs are very useful to understand the progress of Maximum Integrated Intensity along time-points, since they summarize the essential information needed to correctly estimate S-phase duration. In order to eliminate some artifacts, the values of Maximum Integrated Intensity used for tracing these graphs were the values which correspond to a fraction of 0,98 EdU-positive cells. The value of 0,98 was selected and not 1 in order to eliminate a minor fraction of cells with unusually high values of intensity. These latter cells most likely correspond to artifacts, either biological (eg polyploid, giant cells, clusters of cells) or technical. In fact, different experiments present different ranges of intensities. In order to analyze the experiments, namely their behavior along time-points, the values of maximum intensities were normalized for a maximum value of 300.

In 12 experiments, 8 clearly reached maximum EdU intensity between T6h and T7h (experiments 2,3,4,6,7,9,10 and 12), showing that values for maximum EdU-coupled fluorescence intensity pratically stabilized until the T8h time-point was reached; in 3 experiments (experiments 5, 8 and 11) stabilization was achieved between T6h and T7h, however this was not maintained between T7h and T8h; and in 1 additional experiment (experiments 1) intensity values did not stabilize, presenting a linear progress of Maximum Integrated Intensity over time. Figure 3-1 represents the graph with the average values and respective standard deviations for each time-point, of experiments that reached maximum fluorescence intensity between T6h and T7h. The observed stabilization of fluorescence intensities between T6h and T8h means that maximum intensity was achieved, at least for the subset of cells that incorporated EdU for the whole S-phase, after a minimum of 6hours of EdU incorporation. A higher temporal resolution would require incorporation times with shorter increments of EdU pulsing time. However, this still provides a good approximation since analyzing the data on figure 3-1 it is clear that in T7h maximum intensity was already reached. This means that the duration of S-phase is between 6-7h. This result is in close agreement with previously published data for this cell line (HCT-116)[22]. The values for standard deviations, which represent how much the values of each experiment differ from the mean value, are low suggesting good consistency between experiments.

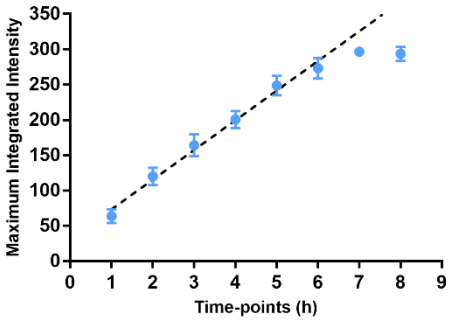

Figure 3-1: Maximum EdU Integrated Intensities vs time-points (experiments 2, 4, 5, 6, 7, 9, 10 and 12; n=8). The tendency line (dashed line) represents the linear increase of maximum Integrated Intensity until T6h. Values displayed as mean ± standard deviation.

3.1.2. IV.1.2.2. Estimation of G1 and G2 phases duration times

In order to estimate G1 and G2-phases duration times, whole DNA staining in addition to EdU staining was performed with DAPI, Hoechst or PI (experiments 5-12). The relative distribution of cells along the different stages of the cell cycle can be easily appreciated in “cell cycle curves” obtained by flow cytometry that depict relative amounts of DNA, i.e. 2n, 4n and intermediate between 2n and 4n[18]. Cell cycle curves similar to those seen by flow cytometry can also be obtained by microscopy (Figure 3-2).

The durations of G1 and G2 phases can be estimated from the dynamics of disappearance of the corresponding peaks in the population of cells that remains EdU-negative with increasing pulsing times with EdU. Indeed, over time, EdU-negative cells in G2 (4n DNA content) enter G1 (2n DNA) stage of the next cell cycle leading to a progressive exhaustion of the G2 peak. Then, expectedly, the EdU-negative G1 peak subsides later, over a period corresponding to the sum of G1 plus G2 phases. In this way it is possible to quantify durations (in units of time) of G2 and G1 plus G2 phases, with the duration of G1 being obtained by inference i.e. by subtracting the duration of G2 phase from the total time that the G1 peak takes to disappear (since the beginning of EdU incorporation) [22].

The quantification of the duration of G1 and G2 phases was performed in 5 experiments: 7, 8, 9, 11 and 12. Of note, experiments 11 and 12 have 10 time-points instead of 8. It is important to mention that in experiments 5 and 6, in which whole DNA was stained with PI, a double peak could not be obtained,

probably due to a problem of bleed-through between channels [30]. Consequently, the quantification of these experiments did not proceed. Since results obtained with DAPI and Hoechst did not present this problem, and their handling did not require the extra step of using Rnase to digest RNA, no additional experiments were done using PI. In addition, the quantification of G1 and G2-phases of experiment 10 was not performed, because the set of input images presented an unusual blurring. Although this did not affect S-phase quantification, it did not allow an accurate identification of whole cells in order to perform the required elimination of EdU-negative cells. In this case, the blurring probably originated during the procedure of mounting the microscope coverslips in anti-fading medium.

The critical step in this procedure was the correct elimination of EdU-negative cells. During this project the strategy used to calculate the threshold value was *Manual*, allowing the estimation of the best threshold values specific for each time-point since each one features a different set of intensities of EdU-coupled fluorescence. As mentioned, these values were established in Preliminary Project. Main project was dived in two parts. Since the main goal of part 1 was the total identification of cells in each channel to completely eliminate cells stained with EdU, the range of typical diameter of nuclei chosen was larger than the one in the project used for S-phase quantification. In addition, method for distinguish clumped objects and draw dividing lines between them was *Intensity* instead of *Shape*, since *Intensity* performs better at distinguishing clumped objects. This can lead to the presence of giant cells or cell clustering on final images of part1, however this will not represent an issue. Indeed, such types of objects will not be identified in part 2 because the diameter returns to a restricted range, and the method used to distinguish clumped objects and draw dividing lines between was, again, *Shape*.

The progression of G1 and G2 cells at successive time-points was evaluated by careful analysis of the corresponding histograms. It was clear that the G2 pick disappeared in all experiments (7, 8, 9, 11 and 12) between time-points T4h and T5h of EdU incorporation, consistent with a duration of 4-5h for G2 phase and in close agreement with previously published data for this cell line (HCT-116) [22]. However, this was not so clear with respect to G1 pick. Disappearance of the G1 peak was not easy to appreciate, due to a decrease of cell number in higher time-points, showing up as a progressively less well defined shape of the histograms. In order to better analyze the data present on histograms, the percentages of cells in G1 and G2 (%G1_tp and %G2_tp) in the total population were estimated for each time-point, based on the percentage of cells within each peak (%G1_pick and %G2_pick), the number of EdU negative cells and the total population. To estimate %G1_tp:

$$NG1 = \%G1\_pick \times (Number\ of\ EdU\ negative\ cells) \quad (1)$$

$$\%G1\_tp = \frac{NG1}{Total\ population} \quad (2)$$

Where NG1 is the number of cells in G1.

The percentage of cells in G1 and G2 were obtained in the .txt file CellCycle_Percentages_table, after running R code with the required input data which in this case was the range of intensities belonging to each pick. This range was selected after analyzing each histogram, taking into account the presence of a given background level. Since the typical shape of the cell cycle curve is lost over time, given the obvious (and expected) decline of EdU-negative cells, the values of more advanced time-points were chosen based on previous time-points.

The Figures 3-2 and 3-3 depict the average percentages of G1 and G2 cells respectively in the total population along time-points of experiments 7,8 and 9, and respective standard deviations (SD). The results of experiments 11 and 12 are not presented together with experiments 7, 8 and 9, since experiments 11 and 12 have two additional time-points. Figures 3-4 and 3-5 depict as well the average percentages of G1 and G2 cells respectively in the total population along time-points, but regarding experiment 11 and 12.

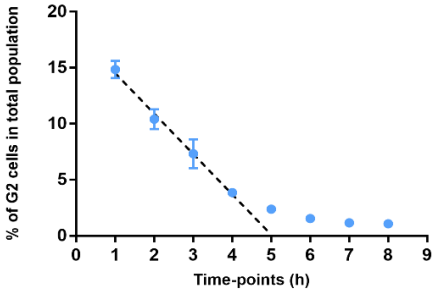

Figure 3-2: Percentages of G2 cells in total population along time-points (experiments 7, 8 and 9; n=3). The tendency line (dashed line) represents the linear decrease of the percentage G2 cells in total population until T4h; Values displayed as mean ± SD

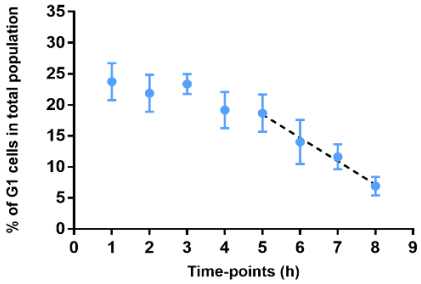

Figure 3-3: Percentages of G1 cells in total population along time-points (experiments 7, 8 and 9; n=3). The tendency line (dashed line) represents the linear decrease of the percentage of G1 cells in total population since T5h; Values displayed as mean ± SD.

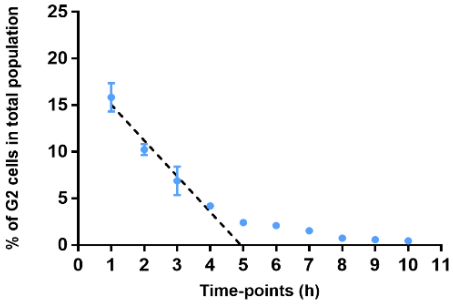

Figure 3-4: Percentage of G2 cells in total population vs time points (experiments 11 and 12; n=3). Values displayed as mean ± SD.

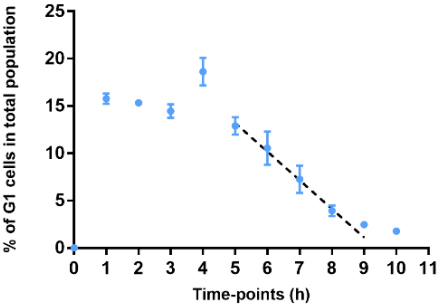

Figure 3-5: Percentage of G1 cells in total population vs time points (experiments 11 and 12; n=3). Values displayed as mean ± SD

Regarding Figures 3-2 and 3-4, the percentage of cells in G2 in total population shows a decline until T4h/T5h followed by stabilization afterwards. The dashed line is the tendency line, which predicts the linear decrease of the percentage of G2 cells along those time-points and emphasizes the stabilization trend that follows after time point T5h. In addition, the values of standard deviations are low meaning that the actual values do not differ much from mean values. This indicates that G2 phase lasts approximately 4-5h. These data are in agreement with our predictions and with published data on features of the cell cycle in this cell line (HCT-116)[22]. Regarding Figures 3-3 and 3-5, their values are more divergent (specially figure 3-3), presenting larger standard deviations. Besides that, the results of experiments 7, 8 and 9 suggested that 8 time-points may not be ideal for quantifying the length of G1 plus G2, since the final stabilization expected was not observed. The results of experiments 11 and 12 show a stabilization after T9h, indicating that the sum of G1 plus G2 is approximately 9h. The duration of G1 phase was estimated by subtracting the duration of G2 phase from the total time that the G1 peak takes to vanish (~9hours in both experiments). So, the length of G1-phase is between 4 and 5 hours. The values obtained for G1 and G2 durations are in agreement with those obtained in the original research where the E-CFI method was established, for the same cell line: 5.4 ± 0,94 h and 3.8 ± 0.45 h for G1 and G2 phases respectively[22]. Further experiments with 10 time-points - need to be performed in order to support the results of the two experiments referred above, and prove the reproducibility of this tool for quantifying not only S-phase but also G1 and G2-phases.

3.1.3. Influence of cell number in the estimation of S phase duration time

Experiment 4 was used to test the influence of number of cells, on S-phase quantification, using different sets of input images (2, 4, 6, 9, 12 and 18), using Project 1 with exactly the same setting as in 3.1.1. Figure 3-6 depicts the maximum Integrated Intensity along time-points using different sets of input images.

It is clear that the typical stabilization between T7h and T8h occurs even when the number of input images is only two. However, the values of the preceding time-points are quite divergent. When sets with less than 9 images were used there was not the increase of the maximum intensity between time-points T4h and T5h, as expected. So, just sets of 9 images or more provide a consistent and reliable result.

3.1.4. Influence of cell number in the estimation of G1 and G2 duration time

Different sets of input images (2, 4, 6, 9 and 12 images) from experiment 7 were used to test the influence of the number of cells on the estimation of G1 and G2 duration times. It is crucial that cell cycle curves present a defined shape, since one of the important steps during G1 and G2 quantification is the selection of the range of intensities belonging to each pick through analysis of the histograms. Two time-points (T1h and T4h) were analyzed with the sets of input images indicated. After obtaining the histograms, it was clear that histograms obtain from only 2 input images did not feature a defined shape. Regarding histograms obtained from 4 and 6 input images, their shape seems to be much more defined, although not as well defined as histograms obtained from 9 or 12 input images. So we cannot claim that this number of input images is enough to correctly select the range of intensities corresponding to each peak. The histograms obtained from 9 input images were very similar with the ones obtained with 12 input images. In addition, the number of cells identified on T4h was 898, which is almost double the number of cells identified for the same time-point when 6 input images were used. In this case seems that 9 images are enough to obtain an accurate selection of the range of intensities (in both time-points T1h and T4h) corresponding to G1 and G2 peaks. These finding are in agreement with the ideas of Roukos and colleagues, which stated that the minimum number of cells needed to quantify cell stages is 500; however higher numbers of cells originate smoother and more accurate cell cycle profiles[21].

3.1.5. Estimation of S phase duration time using Spinning Disk confocal microscopy

The quantification of S-phase using SD confocal microscopy is relevant to prove the applicability of the E-CFI protocol using different microscopies. For this purpose, three experiments (13, 14 and 15) were performed. Project 1 was used as well to process the images obtained from SD confocal microscopy. Resolution and pixel size of widefield microscope and SD confocal microscope are different, so the typical diameter of identified cells had to be adapted for a smaller range (10-25), because with a larger pixel size a smaller number of pixels is needed in order to identify the same area (pixel sizes of widefield and SD confocal microscope are respectively 0,227 µm and 0,667 µm).

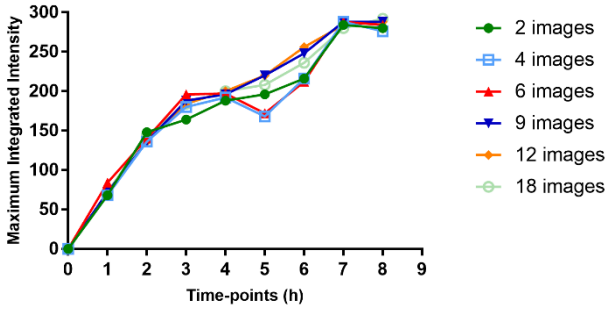

Figure 3-6: Maximum Integrated Intensity along time-points using different sets of input images (2, 4, 6, 9, 12 and 18 images) of experiment 4. Of note, the connecting lines between time-points of experiments are only present to support the data analysis.

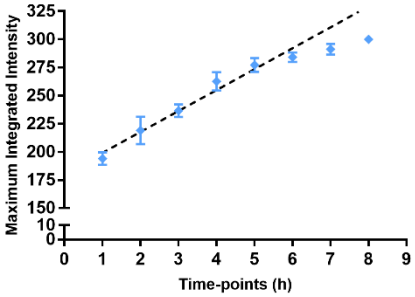

Figure 3-7: Maximum Integrated Intensities along time-points and respective standard deviations (Experiments 13, 14 and 15; n=3). The tendency line (dashed blue line) represents the linear increase of maximum Integrated Intensity until T6h. Orange values highlight the stabilization trend. Values displayed as mean ± standard deviation

The values increase linearly until time-point T6h, although in a smoother way than when using widefield microscopy. Time-point T7h is already significantly below the tendency line (dashed line), meaning that stabilization had already begun. These results are consistent with a duration of S phase of 6-7h. However further experiments need to be done, not only to increase the number of experiments for S-phase quantification, in order to obtain more robust results, but also quantify G1 and G2-phases using this microscopy.

3.1. Hair follicles characterization using EdU

Human hair follicles are in constant cycle, so besides developing a tool for cell cycle quantification using cultured cells, this master thesis aims to establish methodologies for characterizing human hair follicle maintenance and proliferation in vitro, not only qualitatively but also in a quantitative manner. For this purpose, two scalp biopsies were allowed to incorporate EdU for different periods of time - experiment 1 (transplantation biopsy): 12h; experiment 2 (punch biopsy) 4h - in order to analyze the proliferation capacity in four different HF regions namely bulb, sub-bulge (between bulb and bulge), bulge and supra-bulge (between bulge and epidermis). CK-15 was used to assist the identification of bulge region. After image acquisition some of the immunolabeled HF sections were stained with Giemsa, in order to aid in the identification of HF regions during image analysis. So, CK-15 was not used to stain all HF sections.

3.1.1. Qualitative analysis

Before characterizing the dynamics of cell proliferation within HFs it is essential to classify the HFs with respect to their stage within the hair cycle. Distinguishing HFs in anagen from HFs in early catagen is not easy due to their anatomical similarities. A guide to studying human hair follicle cycling developed by Oh and colleagues in 2016 addressed this issue by establishing the key features of human hair follicles during each hair follicle stage. Namely, the “onion” shape of the bulb on anagen VI and the presence of melanin on dermal papilla on early catagen are two useful characteristics for distinguish these two hair follicle stages[31]. So, the three hair follicles analyzed during this thesis were considered as in anagen VI of hair cycle. After performing a broad analysis of hair follicle images, it was clear that bulb and sub-bulge were the regions which presented the most significant distribution of proliferative cells. In supra-bulge region and epidermis EdU-positive cells were less frequent. In contrast, in bulge region EdU-positive cells were almost absent. It was also observed that, regarding experiments 1 and 2, HFs which incorporated EdU for a longer time presented significantly more EdU positive cells, as expected. The observations regarding the bulb and bulge are in agreement with what was expected for anagen VI HFs, since the cycling part of hair follicle, (mainly the bulb region) is the one known to present the larger frequency of proliferative cells[24]. In fact, matrix is colonized by transit amplifying cells with origin in HFSCs, that proliferate and give rise to the inner root sheath and the hair shaft Furthermore, some researchers observed (in mouse models) that ORS progenitors are not the same as IRS and hair shaft progenitors. They describe that ORS progenitors are dispersed along ORS, instead of localized on a niche, promoting a regional growth[32]. Thus, since the ORS is an inward extension of the epidermis with proliferative capacity this result was not unexpected, but we note that quantitative data obtained in human hair follicles is basically non-existent. The sebaceous glands and epidermis also showed some EdU-positive cells. Human skin is in constant renewal and it would thus be expected that the epidermis featured a significant amount of cycling cells[33]. However regarding HF sections of experiment 2, EdU-positive cells in the epidermis occurred mainly on peripheric regions, probably due to the poor penetration of EdU when punch biopsy material (3-4 mm in diameter) was utilized. This was not observed on specimens for HF transplantation (1-1.5 mm diameter).

It is important to mention that, in the context of this thesis work, protocols for sample preparation before cryo-sectioning were also improved. This is relevant since the HF is particularly difficult to section given the coexistence within this mini-organ of structures with highly different stiffness, namely adipose tissue and keratin-rich hair shafts. To this end HFs, either obtained by punch biopsy or isolated HFs obtained in preparation for hair transplantation, were included in acrylamide in order to create a substructure within them. This helped HFs to resist the subsequent step of exposure to a high concentration (8%, w/v) of SDS, in order to retrieve antigens that might be concealed by prolonged formaldehyde fixation.

3.1.2. Quantitative analysis - Bulb and Sub-bulge

Subsequently we quantified EdU incorporation (labeling index), which highlights the presence of cells in S phase or that have recently passed through S phase, in the HF regions that show the highest incorporation of EdU, namely the bulb and sub-bulge ORS regions. For instance, the bulb region was quantified below Auber’s line (AL), above Auber’s line, and in ORS. Three hair follicles in anagen VI were thus quantified, two from experiment 1 (hair follicle #1 and hair follicle #2) and one from experiment 2 (hair follicle #3). Each HF region (bulb and sub-bulge) was quantified using sets of contiguous sagittal or parasagittal images. The number of selected images for each HF area (n) varies depending on the maximum number of sections found reliable for quantification. The cell counter plugin available on *Fiji* was used and different types of counters (or markers) were utilized to distinguish areas within each HF region and for each channel.

The values obatined are depicted on Table 3-1. As expected, in all areas, a higher percentage of EdU-positive cells (Labeling index -LI) was seen in HFs after 12h of EdU incorporation (hair follicles #1 and #2) when compared to a 4h incorporation time (hair follicle #3). In addition, regarding bulb region, the area below AL presented a higher LI than the area above AL. Finally, ORS showed the lowest values, indicating that bulb ORS has low proliferative capacity even in anagen. ORS sub-bulge was quantified not only through the LI but also by estimating the number of EdU-positive cells in a given ORS length (200 micrometers). For this purpose, the length of ORS quantified was measured using *Fiji* features. Both quantifications show a similar pattern between hair follicles. The standard deviations obtained here were slightly larger than the ones obtained in bulb quantification. Actually, the sub-bulge quantification was performed along all ORS. The sections near bulge region, where EdU-positive cells are less abundant, were not analyzed separately from those near the bulb. So, this slightly higher dispersion of values is not surprising.

It is important to mention that, although some research has emerged in the last years using similar methods to study human hair follicle dynamics none presented quantitative data[15]. Also, most of the obtained data on EdU (or BrdU) labeling relates to sub-bulge regions since when using currently available methods HFs

are sectioned at the adipose-dermal transition before culture (amputated HFs)[24].

Table 3-1 EdU-positive cells, LI or number, in HF regions obtained through quantification of n images.

	LI below AL	LI aboveAL	LI in bulb ORS
HF #1 (n=5)	59,6	14,3	2,2
HF #2 (n=4)	57,1	17,2	6,2
HF #3 (n=5)	30,3	5,7	0
Sub-bulge			
	LI in sub-bulge ORS	**Number of EdU-positive cells in 200 µm of sub-bulge ORS**	
HF #1 (n=20)	10,6	6,5	
HF #2 (n=4)	12,3	11	
HF #3 (n=18)	4,1	2,4	

3.2. Preparation of hair follicle cell suspension from human biopsies

The third part of the present master thesis is the initial work of human hair follicles stem cells isolation, which consisted in the optimization of the protocol for preparing hair follicle cell suspension, based on Ohyama et al. (2006) [14] and Hilmi (2013) [26].

The protocol of preparing cell suspensions of HF epithelial cells has two main initial steps, digestion of the connective (including adipose) tissue surrounding HFs and the disruption of epithelial cells from HFs. In the last protocol tested, which is currently in use (Materials and Methods: III-3), we have used collagenase/dispase for connective tissue disruption and trypLE™ Express for disaggregation of epithelial cells from HFs. However, other alternatives have been tested, namely Dispase II (CellnTec) for connective tissue removal and Accutase (CellnTec) or trypsin (Gibco®) for epithelial cell disruption. The times and temperatures of incubation with these enzymes were tested as well. For collagenase/dispase or Dispase II we have tried several combinations such as overnight at 4ºC, overnight at 37ºC and 4h-5h at 37º, and it was established that overnight at 37º was the best choice. In addition, regarding trypLE™ Express or equivalent, after testing times between 20min and 3 hours it was concluded that an incubation of 20-30minutes at 37ºC was enough to disrupt epithelial cells within HFs.

After preparing cell suspensions of HF epithelial cells different culture media were tested such as ProCHO™ 4 medium (04-919Q, Bio Whittaker®, Lonza) and William's E medium GlutaMAX™ (32551020, Gibco®). After several days of culture we observed that cells undergoing proliferation were mainly fibroblasts, not epithelial cells as aimed. By contrast, when HF cellular suspensions were cultured in CnT-07 medium[29] we observed growth of individual colonies comprised of epithelial cells (Figure 3-8).

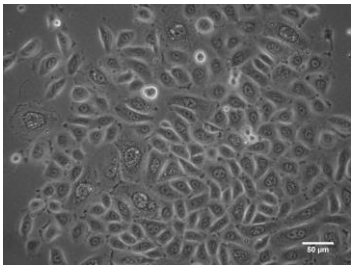

Figure 3-8: Colony of epithelial cells formed after 9 days of culture. Image acquired using the Phase Contrast microscope Zeiss Primovert. Scale:50µm.

4. CONCLUSIONS AND FUTURE TRENDS

Vitiligo is a disease whose pathophysiology remains elusive. A big challenge in this field is how to combine arresting disease progression, that is, promote the transition from active Vitiligo to stable Vitiligo, and at the same time, promote repigmentation of existing lesions. Despite all treatments that developed around the diverse proposed pathophysiologic mechanisms none proved effective[3]. Researchers have developed treatments based on HFSCs, in which cell suspensions are transplanted into Vitiligo lesions (Cellular Grafting), Although results are promising it is felt that much still needs to be done[5].This master thesis aims to contribute to fill in this gap through developing tools for study human HF biology.

In the first part of this thesis, we successfully develop a tool for cell cycle quantification using microscopy. It was obtained a S-phase of 6/7h, a G1-phase of 4/h5 and a G2-phase of 4/5h. In fact, these values are very similar to the results of Pereira and colleagues. They obtained for the same cell line(HCT-116) 6.8 ± 0.35 h, 5.4 ± 0,94 h and 3.8 ± 0.45 for S, G1 and G2 phases respectively[22]. In addition, the influence of cell number was tested and it was concluded that the number of identified cells influences the accuracy of S phase length estimation. Specially in the case of G1 and G, since important step consists in analyzing their peaks corresponding to G1 and G2 stages. So, the number of cells must be enough to originate well defined cell cycle profiles. There must be a balance between the number of images acquired and the time spent acquiring and processing the data, since a higher number of images, giving rise to a larger number of identified cells, originate better defined cell cycle profiles but is more time consuming. Finally, the results obtained using images acquired on SD confocal microscopy corroborate the results using widefield microscopy indicating that the tool developed in this master thesis for cell cycle quantification can be adapted for different microscopies. As mentioned before, this year Ferro and colleagues also reported the use of microscopy to acquire DNA content but using a different method for image analysis. More specifically they quantified the percentage of cells on each cell cycle stage[23]. Since they used a different cell line, the values obtained cannot be compared, however this study is an evidence that cell cycle quantification using microscopy has been a focus of studies of numerous investigators in the past few year.

In the second part of this thesis, human HFs were characterized regarding their maintenance and proliferation capacity in vitro. In sum, in this work conditions for culture and metabolic labeling (deoxy-nucleotide/EdU incorporation) of entire HFs, for improving cryo-sectioning of human HFs and for quantitation of EdU-labeled cells across different sub-regions of HFs have been established. As expected, the bulb region showed the highest labeling index, but proliferation in outer root sheath cells was also documented and quantified. Since quantifications for the same HF were performed in contiguous sections this strongly suggests intrinsic robustness and high uniformity in cell counting procedures. This will predicate development of future research utilizing HFs in the recipient laboratory.

The third part of this thesis corresponds to the initial steps towards isolation of HF stem cells. After a process of optimization, we obtained cultures of HF epithelial cells that grow robustly using Cnt-07 medium. These cells are in the process of expansion before

checking for the presence of cytokeratin 15 (CK15) and the cell surface antigen CD200, both markers of bulge HFSCs[13][14].

In conclusion, the tools developed during this master thesis research will be useful for studying the proliferation of cell populations within human HFs including HFSCs, generating relevant knowledge to be subsequently applied to the study of disorders such as Vitiligo.

ACKNOWLEDGMENTS

I would like to thank my supervisors Professor João Ferreira, professor Cláudia Lobato da Silva and Professor Paulo Filipe.

REFERENCES

[1] A. Alikhan, L. M. Felsten, M. Daly, and V. Petronic-Rosic, "Vitiligo: A comprehensive overview: Part I. Introduction, epidemiology, quality of life, diagnosis, differential diagnosis, associations, histopathology, etiology, and work-up," *J. Am. Acad. Dermatol.*, vol. 65, no. 3, pp. 473–491, 2011.

[2] A. Taieb *et al.*, "Guidelines for the management of vitiligo: The European Dermatology Forum consensus," *Br. J. Dermatol.*, vol. 168, no. 1, pp. 5–19, 2013.

[3] N. van G. khaled Ezzedine, Viktoria Eleftheriadou, Maxine Whitton, "Vitiligo," *Lancet*, pp. 74–84, 2015.

[4] L. M. Felsten, A. Alikhan, and V. Petronic-Rosic, "Vitiligo: A comprehensive overview: Part II: Treatment options and approach to treatment," *J. Am. Acad. Dermatol.*, vol. 65, no. 3, pp. 493–514, 2011.

[5] K. Vinay and S. Dogra, "Stem cells in vitiligo: Current position and prospects," *Pigment Int.*, vol. 1, no. 1, pp. 8–12, 2014.

[6] G. Cotsarelis, T. T. Sun, and R. M. Lavker, "Label-retaining cells reside in the bulge area of pilosebaceous unit: Implications for follicular stem cells, hair cycle, and skin carcinogenesis," *Cell*, vol. 61, no. 7, pp. 1329–1337, 1990.

[7] J. Cui, L. Y. Shen, and G. C. Wang, "Role of hair follicles in the repigmentation of vitiligo.," *The Journal of investigative dermatology*, vol. 97, no. 3. pp. 410–6, 1991.

[8] A. N. Mull, A. Zolekar, and Y. Wang, "Understanding Melanocyte Stem Cells for Disease Modeling and Regenerative Medicine Applications," no. December, pp. 30458–30469, 2015.

[9] S. Mohanty, A. Kumar, J. Dhawan, V. Sreenivas, and S. Gupta, "Noncultured extracted hair follicle outer root sheath cell suspension for transplantation in vitiligo," *Br. J. Dermatol.*, vol. 164, no. 6, pp. 1241–1246, 2011.

[10] A. A. Panteleyev, "Putting the human hair follicle cycle on the map," *J. Invest. Dermatol.*, vol. 136, no. 1, pp. 4–6, 2016.

[11] L. Alonso and E. Fuchs, "Stem cells of the skin epithelium," *PNAS*, vol. 100, pp. 11830–11835, 2003.

[12] A. Kumar, S. Mohanty, S. Gupta, and P. Sm, "Stem Cells of the Hair Follicular Tissue : Application in Cell Based Therapy for Vitiligo," *Hair Ther. Transplant.*, vol. 5, no. 1, pp. 1–5, 2015.

[13] S. Lyle, M. Christofidou-Solomidou, Y. Liu, D. E. Elder, S. Albelda, and G. Cotsarelis, "The C8/144B monoclonal antibody recognizes cytokeratin 15 and defines the location of human hair follicle stem cells," *J. Cell Sci.*, vol. 111, pp. 3179–3188, 1998.

[14] M. Ohyama *et al.*, "Characterization and isolation of stem cell–enriched human hair follicle bulge cells ," vol. 116, no. 1, 2006.

[15] T. S. Purba, L. Brunken, N. J. Hawkshaw, M. Peake, J. Hardman, and R. Paus, "A primer for studying cell cycle dynamics of the human hair follicle," *Exp. Dermatol.*, vol. 25, no. 9, pp. 663–668, 2016.

[16] J. A. McGrath, J. Uitto, and F. M. Pope, "Chapter 3: Anatomy and Organization of Human Skin," in *Rook's Textbook of Dermatology*, Seventh., Wiley-Blackwell, 2004, pp. 1–53.

[17] G. M. Cooper, "The Eukaryotic Cell Cycle," in *The Cell: A Molecular Approach*, Second., 2000.

[18] Z. Darzynkiewicz and X. Huang, "Analysis of cellular DNA content by flow cytometry," *Curr. Protoc. Immunol.*, vol. 5, no. 1, pp. 5–7, 2004.

[19] A. Salic and T. J. Mitchison, "A chemical method for fast and sensitive detection of DNA synthesis in vivo.," *Proc. Natl. Acad. Sci. U. S. A.*, vol. 105, no. 7, pp. 2415–2420, 2008.

[20] H. Zhao *et al.*, "DNA damage signaling, impairment of cell cycle progression, and apoptosis triggered by 5-ethynyl-2′-deoxyuridine incorporated into DNA," *Cytom. Part A*, vol. 83, no. 11, pp. 979–988, 2013.

[21] V. Roukos, G. Pegoraro, T. C. Voss, and T. Misteli, "Cell cycle staging of individual cells by fluorescence microscopy," *Nat. Protoc.*, vol. 10, no. 2, pp. 334–348, 2015.

[22] P. D. Pereira *et al.*, "Quantification of cell cycle kinetics by EdU (5-ethynyl-2′-deoxyuridine)-coupled-fluorescence-intensity analysis," *Oncotarget*, vol. 8, no. 25, pp. 40514–40532, 2017.

[23] A. Ferro, T. Mestre, P. Carneiro, I. Sahumbaiev, R. Seruca, and J. M. Sanches, "Blue intensity matters for cell cycle profiling in fluorescence DAPI-stained images," *Lab. Investig.*, vol. 97, no. 5, pp. 615–625, 2017.

[24] E. A. Langan, M. P. Philpott, J. E. Kloepper, and R. Paus, "Human hair follicle organ culture: theory, application and perspectives," *Exp. Dermatol.*, vol. 24, no. 12, pp. 903–911, 2015.

[25] J. E. Kloepper, K. Sugawara, Y. Al-Nuaimi, E. Gáspár, N. van Beek, and R. Paus, "Methods in hair research: how to objectively distinguish between anagen and catagen in human hair follicle organ culture," *Exp. Dermatol.*, pp. 305–312, 2009.

[26] A. B. M. Hilmi *et al.*, "A simple culture method for epithelial stem cells derived from human hair follicle," *Cent. Eur. J. Biol.*, vol. 8, no. 5, pp. 432–439, 2013.

[27] "CellProfiller Software." [Online]. Available: cellprofiler.org. [Accessed: 23-May-2017].

[28] "CellProfiller Manual." [Online]. Available: http://cellprofiler.org/manuals/current/. [Accessed: 22-May-2017].

[29] "CellnTec: Cnt-07 media." [Online]. Available: http://cellntec.com/products/cnt-07/. [Accessed: 17-Oct-2017].

[30] M. Abramowitz, B. Herman, D. B. Murphy, and M. W. Davidson, "Olympus: Anatomy of the Fluorescence Microscope." [Online]. Available: https://www.olympus-lifescience.com/en/microscope-resource/primer/techniques/fluorescence/anatomy/fluoromicroanatomy/. [Accessed: 07-Oct-2017].

[31] J. W. Oh *et al.*, "A guide to studying human hair follicle cycling in vivo," vol. 136, no. 1, pp. 34–44, 2016.

[32] E. Legué and J.-F. Nicolas, "Hair follicle renewal: organization of stem cells in the matrix and the role of stereotyped lineages and behaviors.," *Development*, vol. 132, no. 18, pp. 4143–4154, 2005.

[33] G. Cotsarelis, "Epithelial stem cells: a folliculocentric view.," *J. Invest. Dermatol.*, vol. 126, no. 7, pp. 1459–1468, 2006.